



Evaluation of the Precision in Level 2 VIIRS and AVHRR Sea Surface Temperature Fields

Fan Wu^{⌘ §}, Peter Cornillon[§], Lei Guan[⌘], Brahim Boussidi[§]

⌘ : Ocean University of China, § : University of Rhode Island

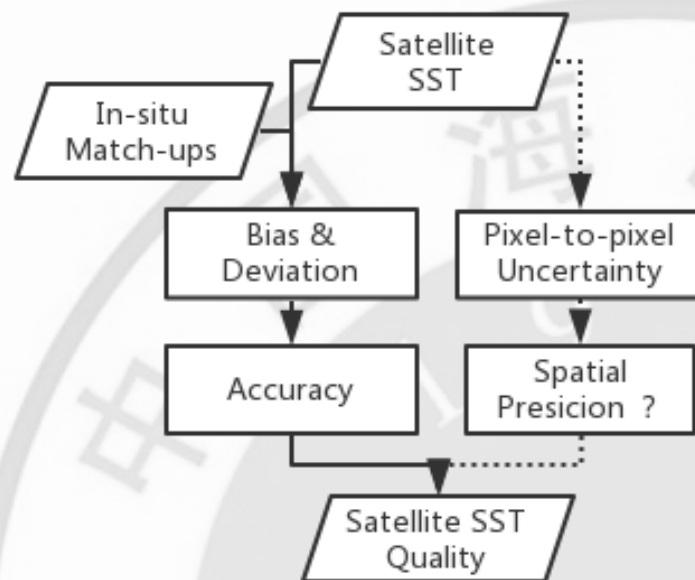


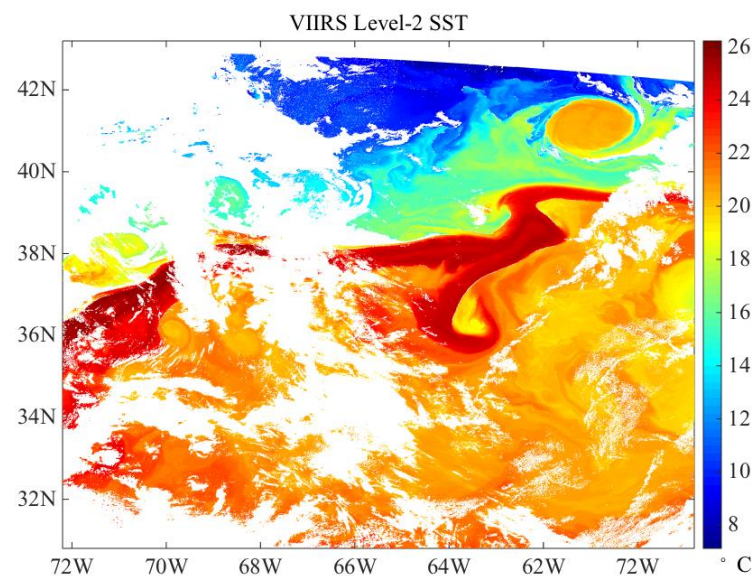
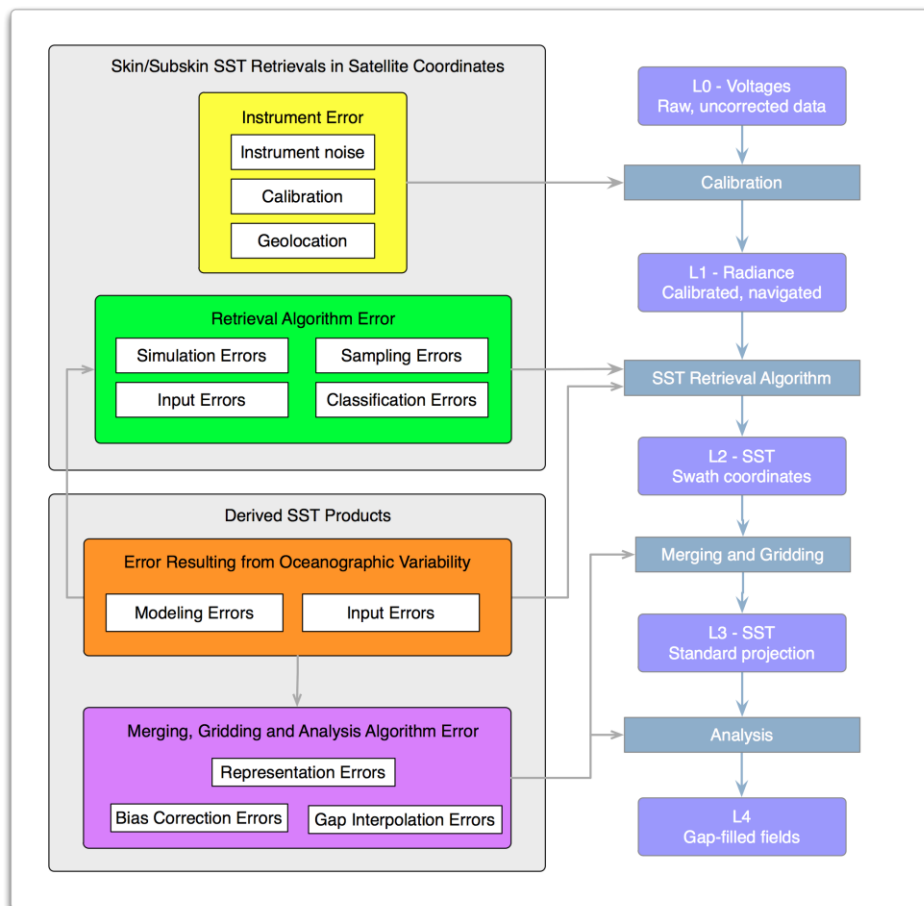
1 Introduction

1.2.2 Satellite SST Spatial Precision

The quality of a complete 2-dimension satellite-derived product include two measure :

- 1 Accuracy: the measure to the absolute error of the product parameter, the uncertainty of the retrieved SST relative to the actual SST
- 2 Spatial Precision: the measure to the spatial content quality of the field, the pixel-to-pixel uncertainty in SST in a single image





The error budget developed by the NASA-NOAA SST Science Team for satellite-derived SST fields.

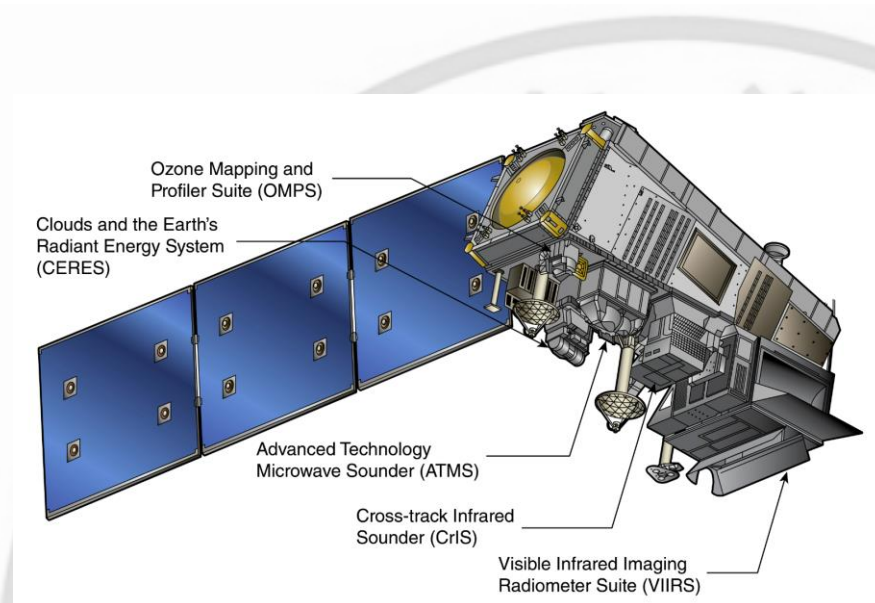


2 Data

2.1 Suomi-NPP/VIIRS SST

Suomi-NPP Parameters

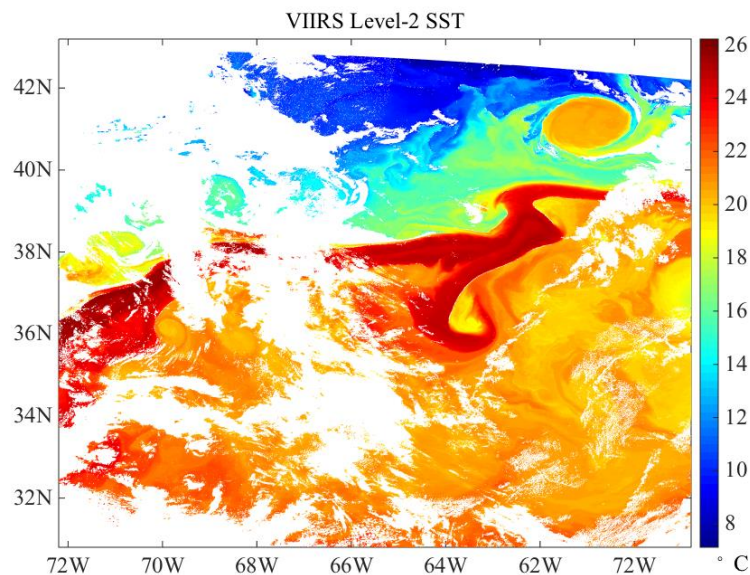
Mission Type	Meteorology	Launch Site	Vandenberg SLC-2W
Operator	NASA/NOAA/ DoD	Reference System	Geocentric
Mission Duration	5 years	Orbit	Polar-orbiting
Launch Mass	2128 kg	Semi-major Axis	7204 km
Payload Mass	464 kg	Perigee	833.7 km
Dmensions	1.3 m × 1.3 m × 4.2 m	Apogee	834.3 km
Launch Date	28 Oct. 2011	Inclination	98.7 °
Rocket	DeltaII 7920-10 D357	Period	101.44 min



Suomi-NPP and the loading



Band	Wavelength (μm)	Application	Band	Wavelength (μm)	Application
M1	0.402 ~ 0.422	Ocean Color, Aerosols	I3	1.580 ~ 1.640	Binary Snow Map
M2	0.436 ~ 0.454	Ocean Color, Aerosols	M10	1.580 ~ 1.640	Snow Fraction
M3	0.478 ~ 0.498	Ocean Color, Aerosols	M11	2.225 ~ 2.275	Clouds
M4	0.545 ~ 0.565	Ocean Color, Aerosols	I4	3.550 ~ 3.930	Imagery Clouds
I1	0.600 ~ 0.680	Imagery	M12	3.660 ~ 3.840	SST
M5	0.662 ~ 0.682	Ocean Color, Aerosols	M13	3.973 ~ 4.128	SST, Fires
M6	0.739 ~ 0.754	Atmospheric Corr'n	M14	8.400 ~ 8.700	Cloud Top Properties
I2	0.846 ~ 0.885	NDVI	M15	10.263 ~ 11.263	SST
M7	0.846 ~ 0.885	Ocean Color, Aerosols	I5	10.500 ~ 12.400	Cloud Imagery
M8	1.230 ~ 1.25	Cloud Particle Size	M16	11.538 ~ 12.488	SST
M9	1.371 ~ 1.386	Cloud Cover			



VIIRS SST Image

The VIIRS Sea Surface Temperature Environmental Data Record (EDR) obtained from:

http://www.nsof.class.noaa.gov/saa/products/search?datatype_family=VIIRS_EDR



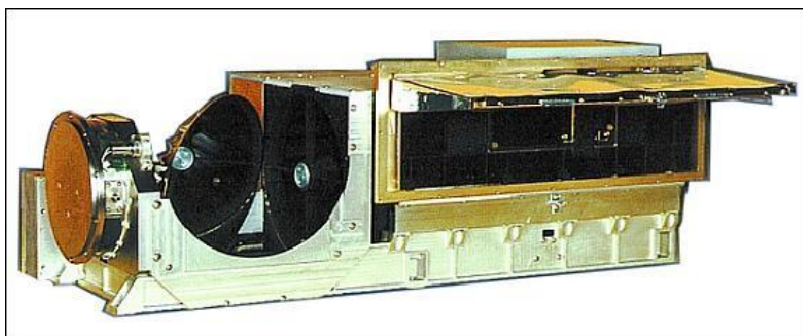
AVHRR, MODIS, VIIRS NETD(Seelye, 2014)

AVHRR Band	Wavelength (μm)	NETD (K)	MODIS Band	Wavelength (μm)	NETD (K)	VIIRS Band	Wavelength (μm)	NETD (K)
1	0.58-0.68		10	0.483-0.493		M4	0.54-0.56	
2	0.725-1.0		16	0.862-0.877		M7	0.85-0.88	
3A	1.58-1.64						1.58-1.64	0.07
3B	3.55-3.93	0.1				14	3.55-3.93	0.07
			20	3.660-3.840	0.05	M12	3.66-3.84	0.04
			22	3.929-3.989	0.07	M13	3.97-4.13	0.08
			23	4.020-4.080	0.07			
4	10.3-11.3	0.1	31	10.78-11.28	0.05	M15	10.3-11.3	0.04
5	11.5-12.5	0.1	32	11.77-12.27	0.05	M16	11.5-12.5	0.07

2.1.2 NOAA/AVHRR SST



NOAA-15



AVHRR/3

AVHRR/3 Band Characteristic

Band	Wavelength (μm)	Nadir Resolution (km)	Angular Resolution (mr)	Scanning Angle (°)	Swath Width (km)
1	0.58 ~ 0.68	1.09	1.4	± 55.4	2700
2	0.725 ~ 1.00				
3A	1.58 ~ 1.64				
3B	3.55 ~ 3.93				
4	10.30 ~ 11.30				
5	11.50 ~ 12.50				

The AVHRR product used was derived with the Pathfinder retrieval algorithm. Retrievals were performed at the University of Rhode Island.



2.2 In-situ Data

- The Oleander project began in 1992 as an effort to conduct high-resolution upper-ocean velocity measurements on a sustained multiyear basis.
- In the past 15 years of this project, upper-ocean velocity and near-surface temperatures have been sampled by an acoustic Doppler current profiler (ADCP), and two mounted in the hull of a container vessel (CMV Oleander) that operates weekly between New Jersey and Bermuda.



CMV Oleander



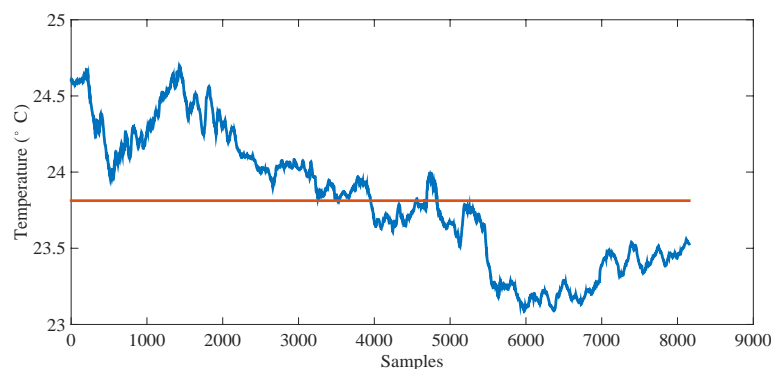
SBE38



- When the speed of the ship is 16 knots, the spatial resolution of TEX is 75 m. TEX data for the period September 2007 to fall 2013 were obtained

SBE38 Parameters

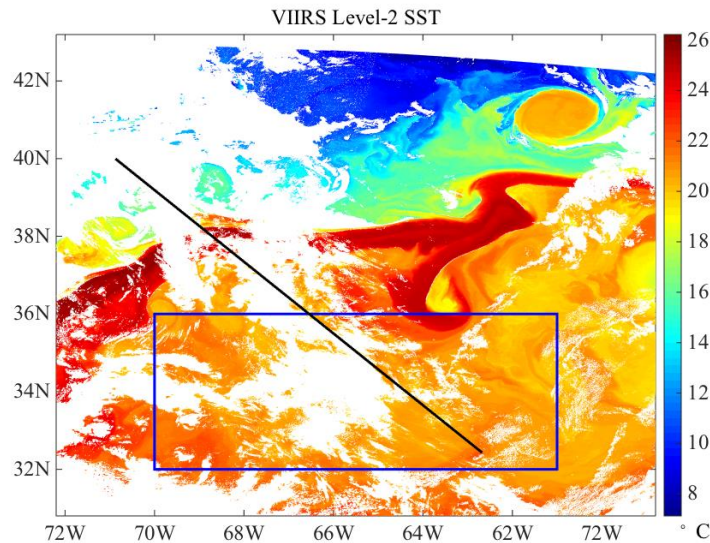
Accuracy (K)	Resolution (K)	Responsible Time (S)	Sample Interval (S)
0.001	0.00025	0.5	10



TEX Data

2.3 Research Area

- Satellite Data Area: 32°N — 36°N , 63°W — 72°W .



Oleander track(black line) and
research area(blue frame)

2.4 The Study Period

The analyses presented here are based on SST fields from the summer of 2012 only – June, July and August because the summer months are substantially less cloud contaminated than the other seasons.



3 Data Preprocessing

3.1 Satellite Data Preprocessing

3.1.1 Data Classification

- Classification:

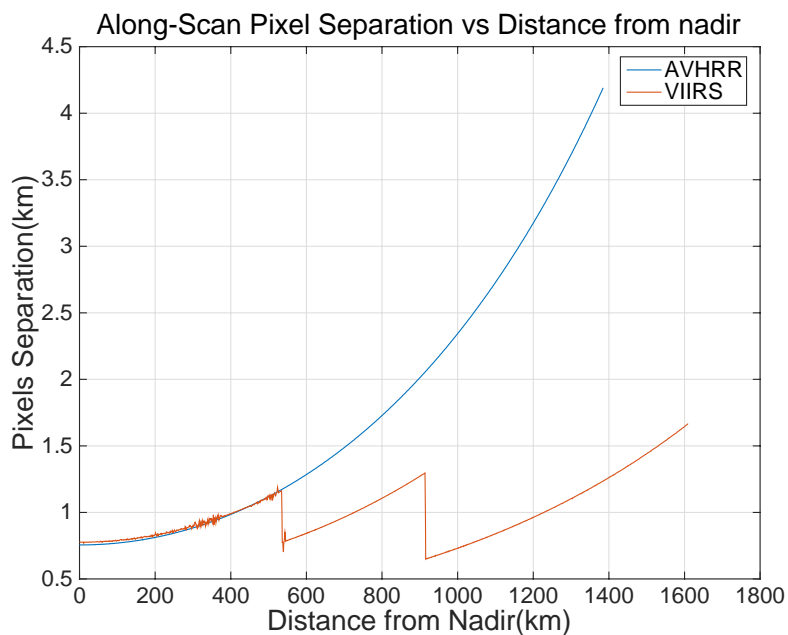
1 The satellite-derived SST fields evaluated here are obtained from scanning radiometers, the characteristics of which may differ in the along-scan versus along-track directions. This is indeed the case for VIIRS due to the use of multiple detectors for each scan, which results in *striping* of the fields (Bouali and Ignatov 2014). The decision was therefore made to separate the data into along-scan and along-track sections.

2 The data were farther divided into day and night fields to allow analysis of the possible effect of diurnal warming on the spectral characteristics of the fields.

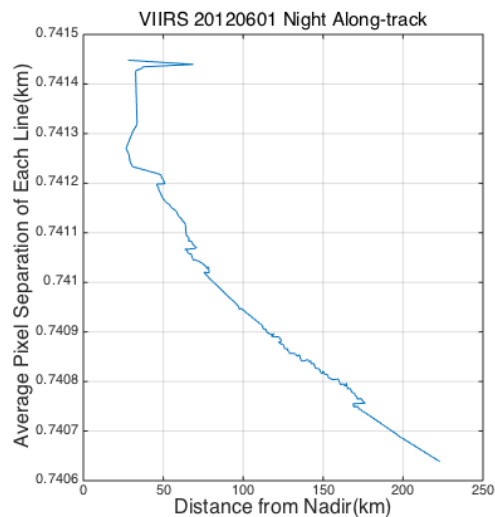
Non-overlapping sections with 256 pixels were selected.



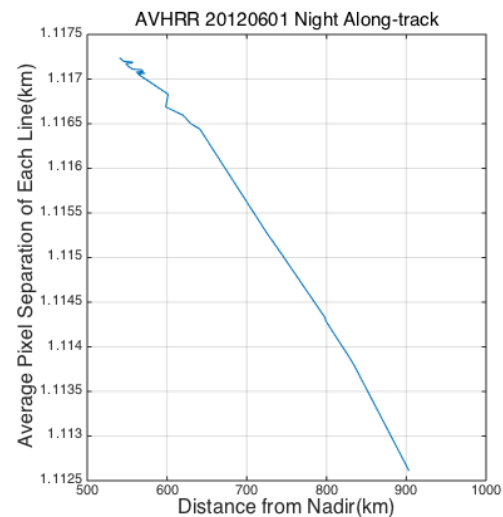
3.1.2 Data Selection



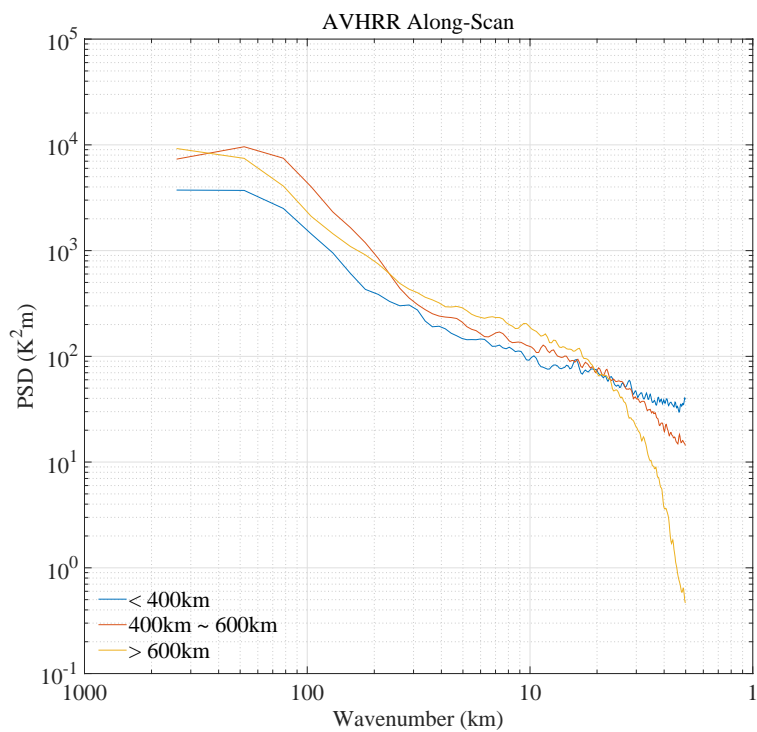
Spacing in the along-scan direction for AVHRR and VIIRS pixels in L2 fields as a function of distance from nadir.



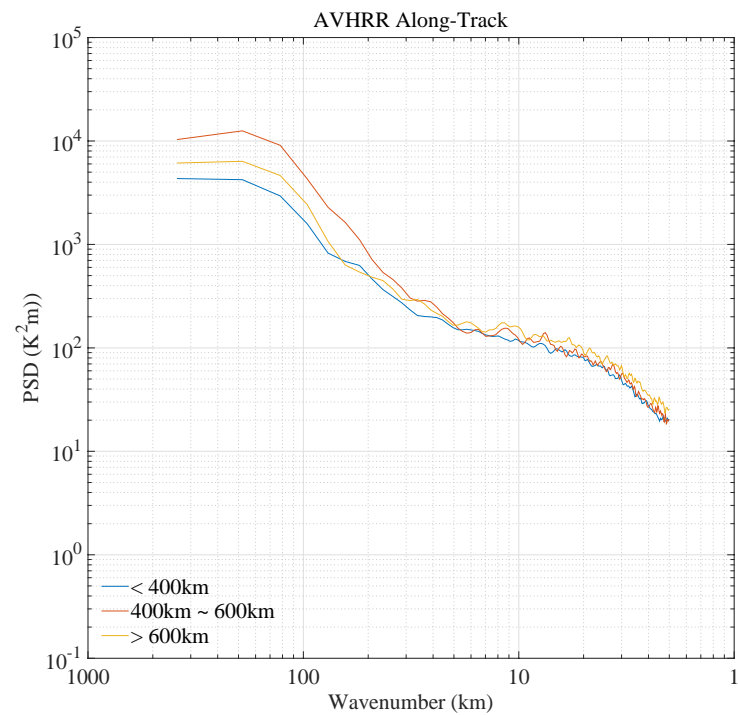
VIIRS Along-track



AVHRR Along-track



Along-scan

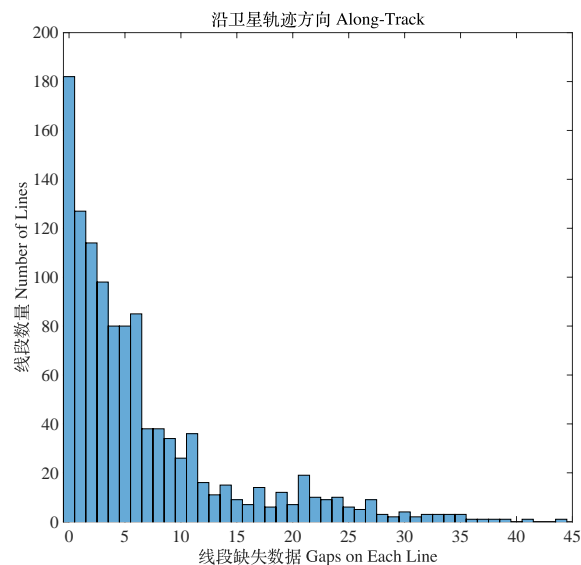
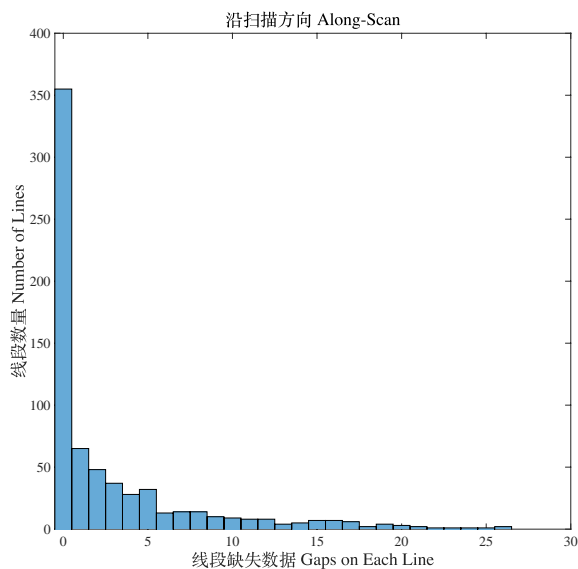


Along-track



3.1.3 Gap Filling

- Gaps were replaced using a Barnes filter if 13 of the 24 pixels in a 5x5 pixel square surrounding the pixel of interest are cloud-free, otherwise the pixel remains flagged as missing. This corresponds to a decay scale associated with the averaging of 1.5 km for VIIRS and 2 km for AVHRR. Following this gap filling, all complete (no missing values) 256 pixel, non-overlapping sections in the along-track direction meeting the distance from nadir criterion were selected as were all non-overlapping along-scan sections. More than 6% of the pixels were filled on <10% sections.

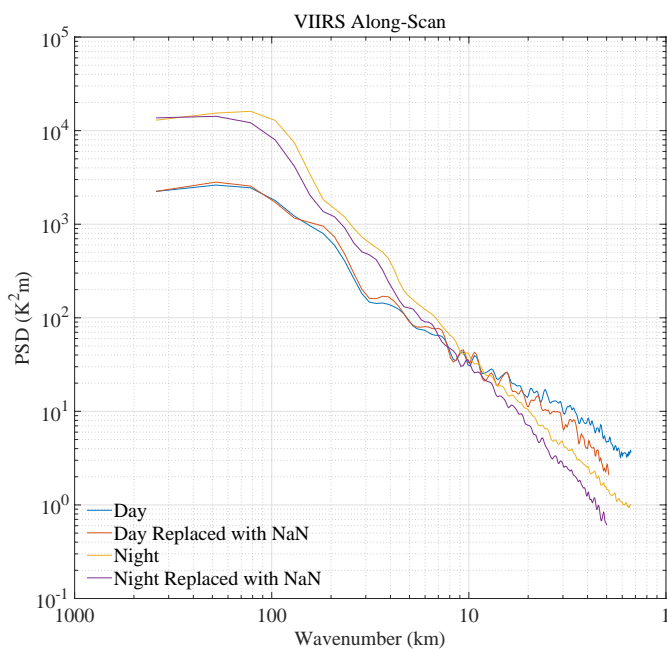


Gaps number in VIIRS sections

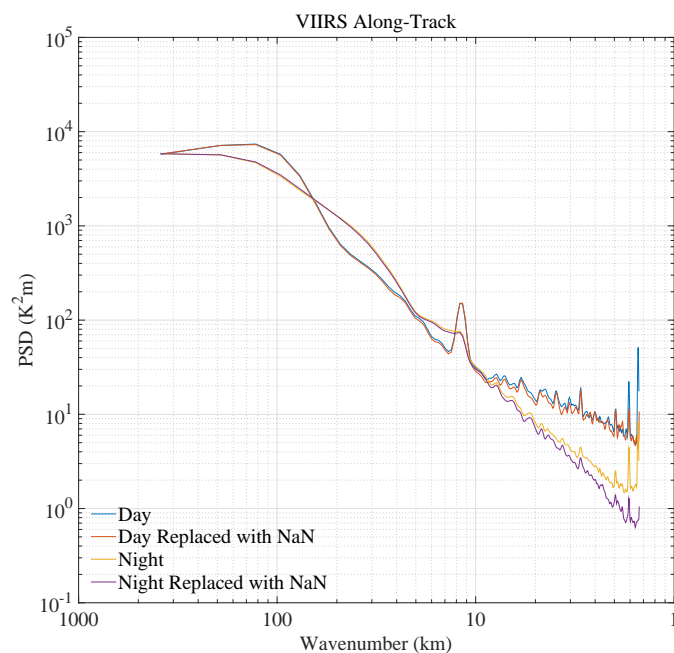


3.1.3 Gap Filling

The impact of gap filling, the “worst case” test.



Along-Scan

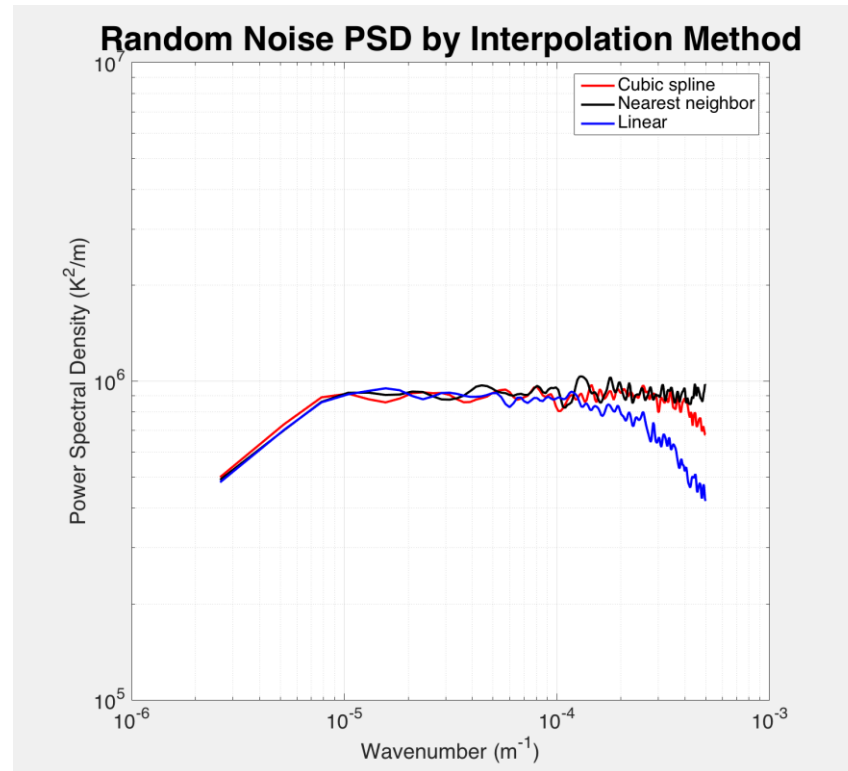


Along-Track

Less than 0.6% of all values contributing were replaced with the Barnes filter.



3.1.4 Interpolation to Equal Spacing



Spectral response of the interpolation methods applied to white noise.



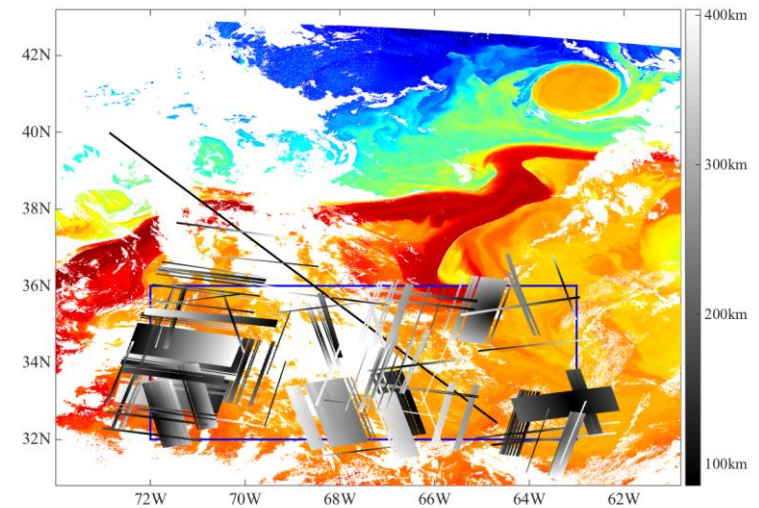
3.1.4 Interpolation to Equal Spacing

Table1 Number of sections meeting the given selection criteria

	Day		Night	
	Along-Scan	Along-Track	Along-Scan	Along-Track
VIIRS - JPSS	126	517	561	615
AVHRR - Pathfinder	266	256	104	193

Table 2 Grouping of along-scan sections based on mean pixel spacing of the temperature section.

	Group 1 (m)	Group 2 (m)	Group 3 (m)
VIIRS	770-805-820	860-885-910	940-995-980
AVHRR	760-765-810	820-865-920	940--947980



location of sections extracted from VIIRS SST fields



3.2 In-situ Data Preprocessing

- The number of Oleander TEX sections for the summers of 2008-2013 is 42.
- MV Oleander crosses the study area: 20 hrs ,
- TEX sample depth : 5 and 6 m below the surface.
- Gap filling : Barnes filtering(decay scale of 0.2 km)

⑩ ↓

- Interpolation to equal spacing: Nearest neighbor interpolated

The mean spacing over all sections: 74.9 m (with a minimum of 74.6 m and a maximum of 75.0 m).



VIIRS SST fields spectra

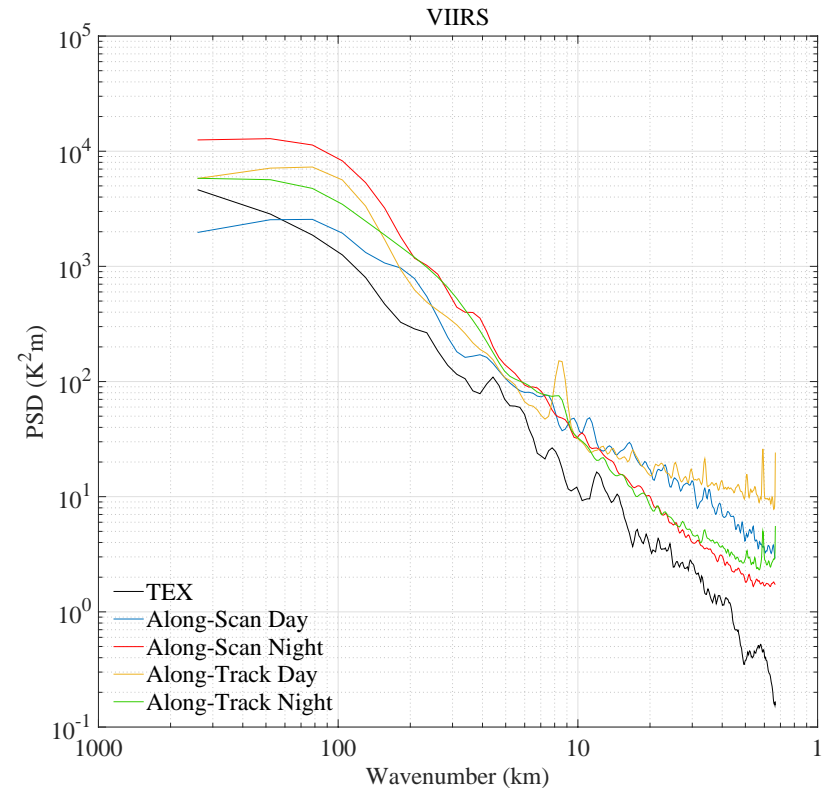
VIIRS night along-scan spectra provide excellent estimates of the slope from 0.75 km ~ 50 km.

Spectra energy: day > night.

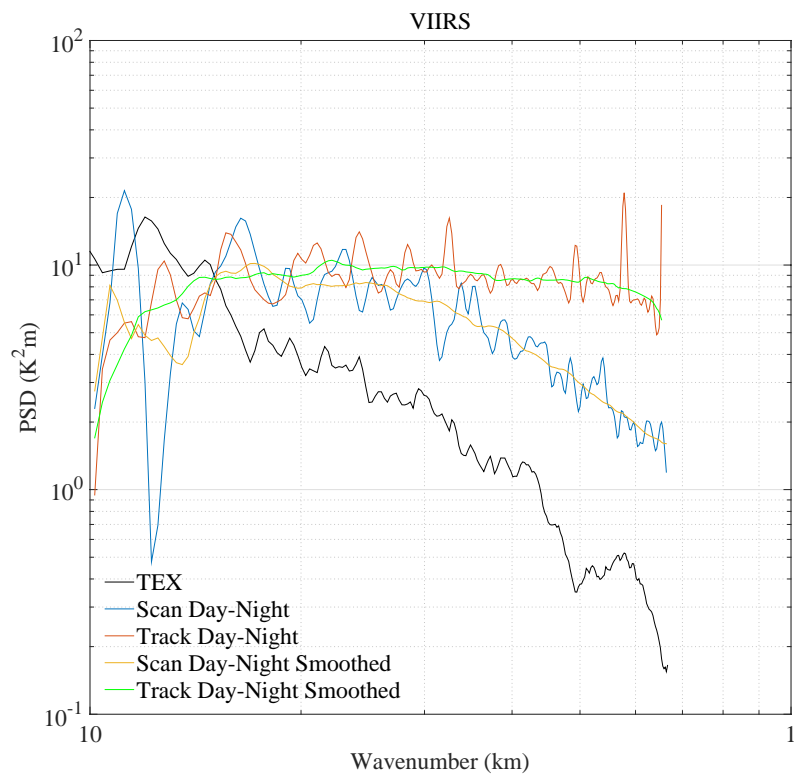
Spectral peaks along-track:

1.5, 2.2, 2.9, 12 km

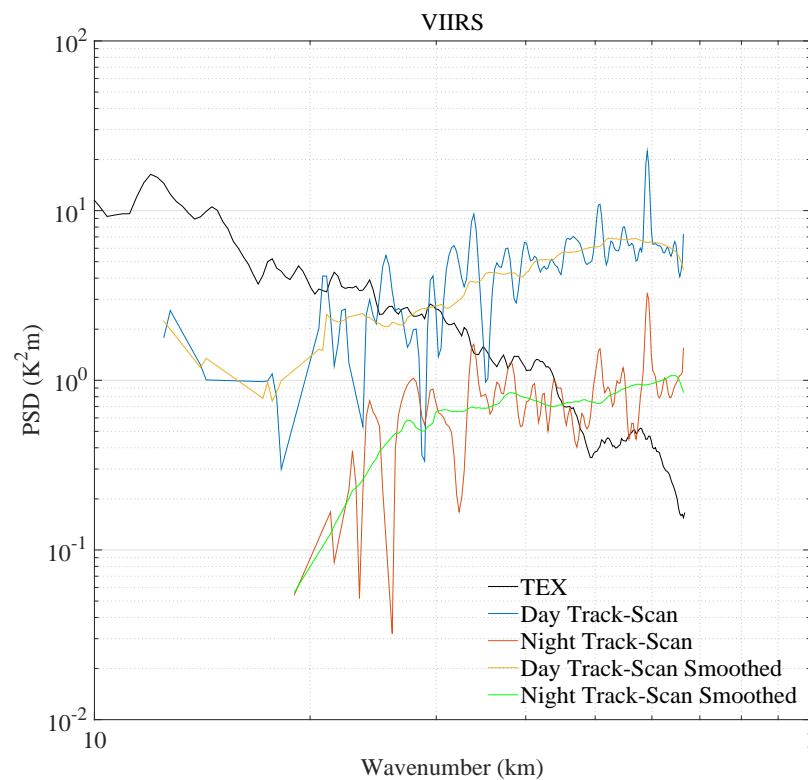
VIIRS spectra are more energetic than the in situ spectrum



VIIRS SST fields Spectra



VIIRS spectra Day – Night

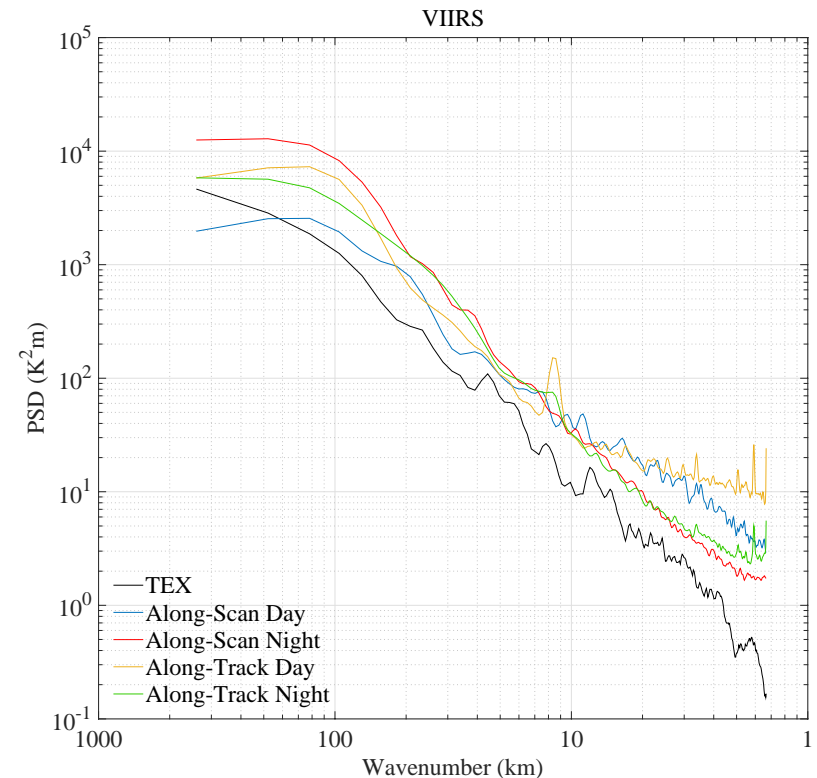


VIIRS spectra along-track – along-scan



VIIRS/TEX spectra energy difference:

- *Satellite-surface vs in situ-approximately 6 m.*
 - *Satellite-averages over regions 750x750 m² vs in situ-averaged over order 10 point samples, an approximately 750 m long section.*
 - *Satellite-sections are closer to meridional and zonal vs in situ-sections trend northwest-to-southeast.*
- {Tandeo:2014ei} and obtained from P. Tandeo, *Anisotropy ratio: ~0.70*, and, both the along-track and along-scan, daytime and night-time spectra are higher than the TEX spectrum.

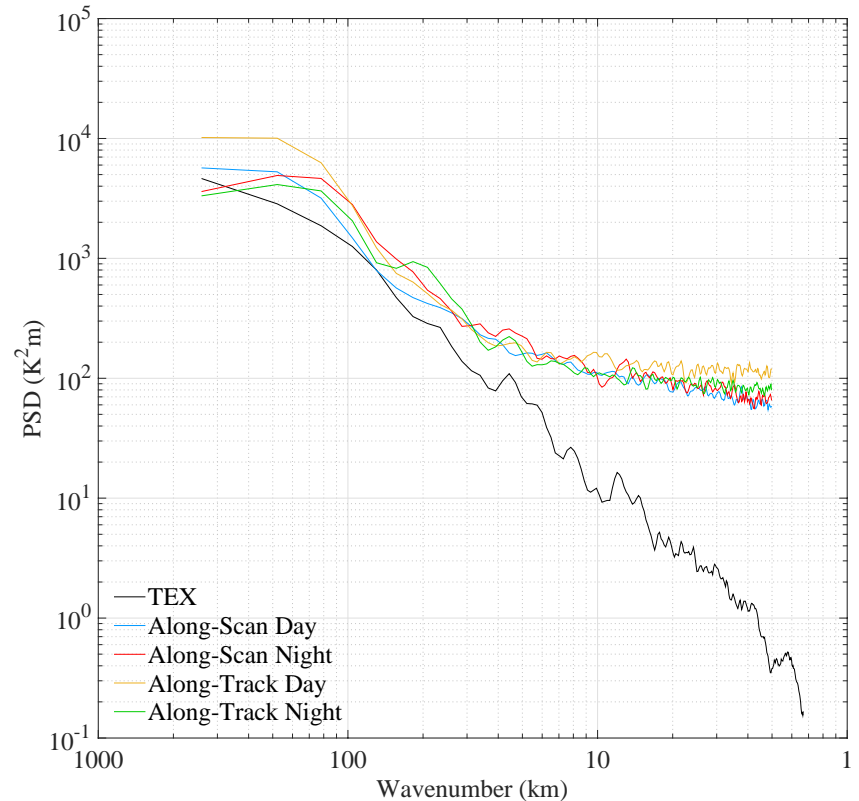


VIIRS SST空间能量谱

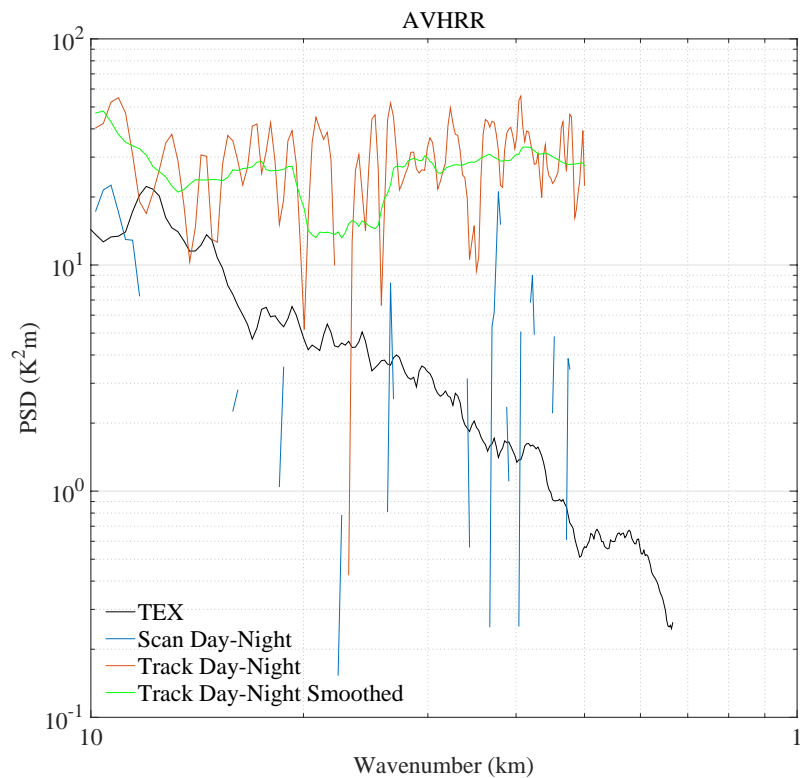


4.3 AVHRR SST Fields Spectra

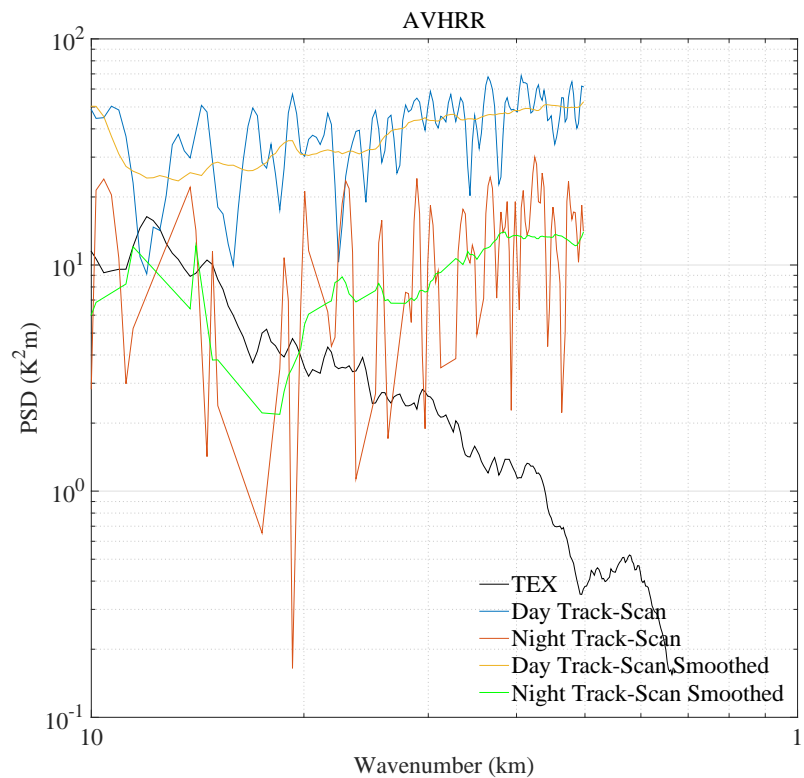
- Elevated energy at scales < 70 km
Levels off at scales < 10 km
- Little difference on energy and slope between the four sets of data.
- The instrument noise associated with the AVHRR overwhelms the day-night spectral differences.



AVHRR SST fields spectra



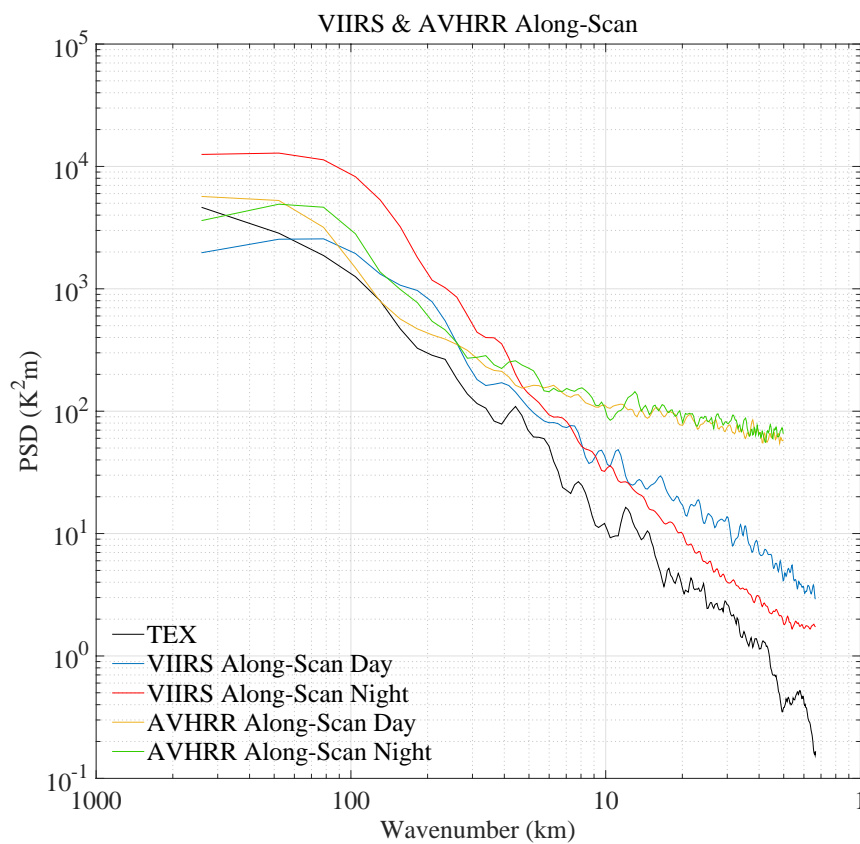
AVHRR spectra Day – Night



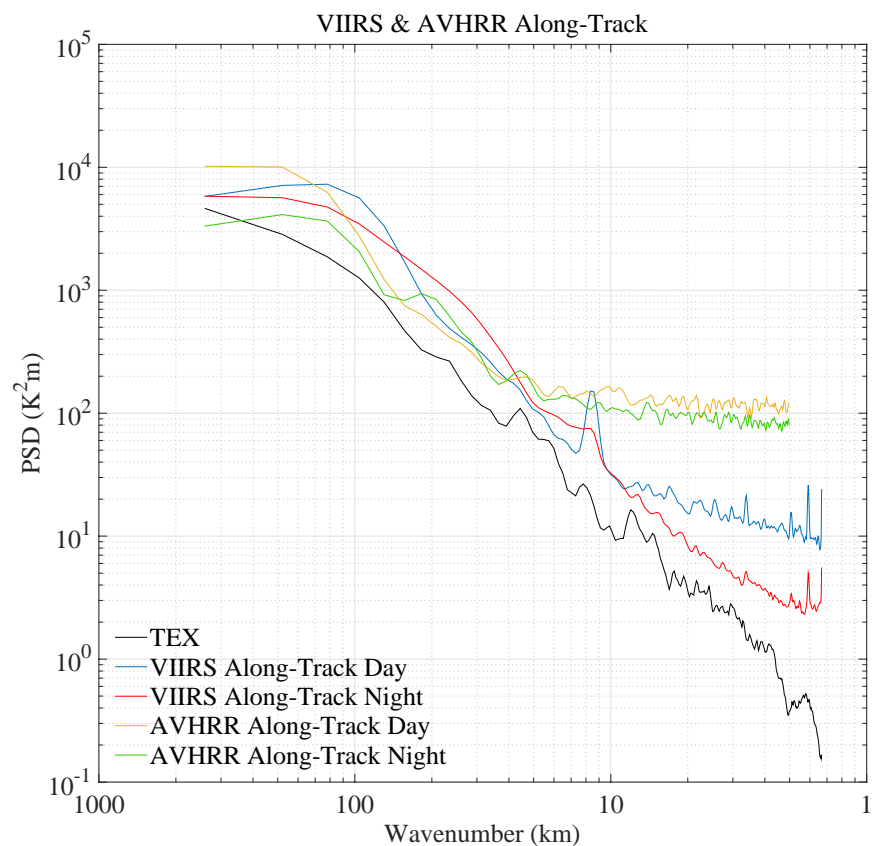
AVHRR spectra along-track – along-scan



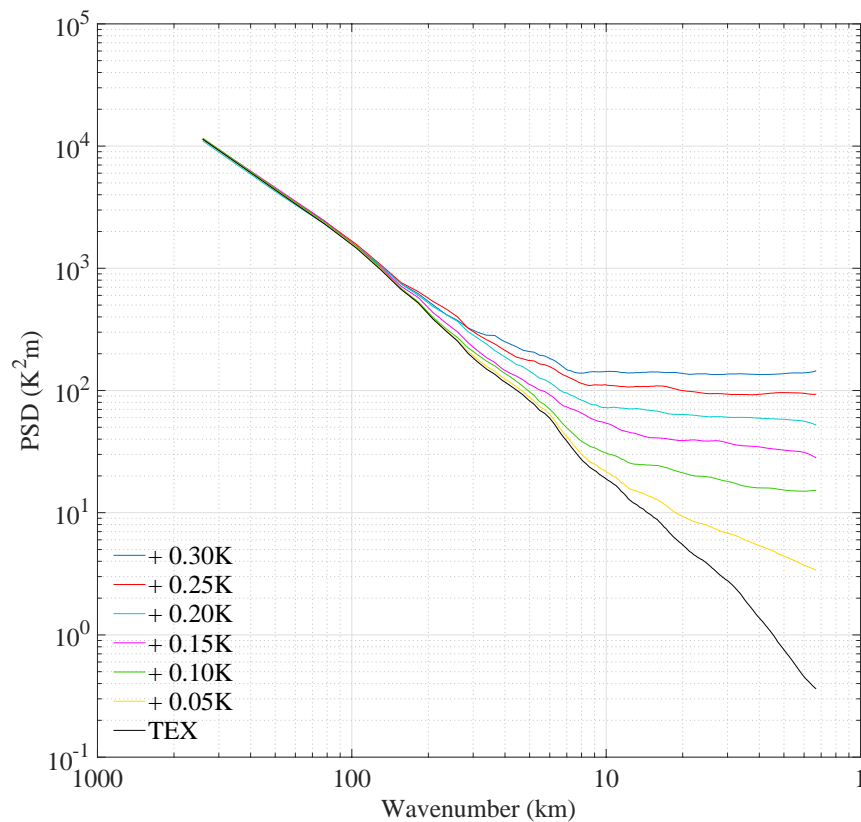
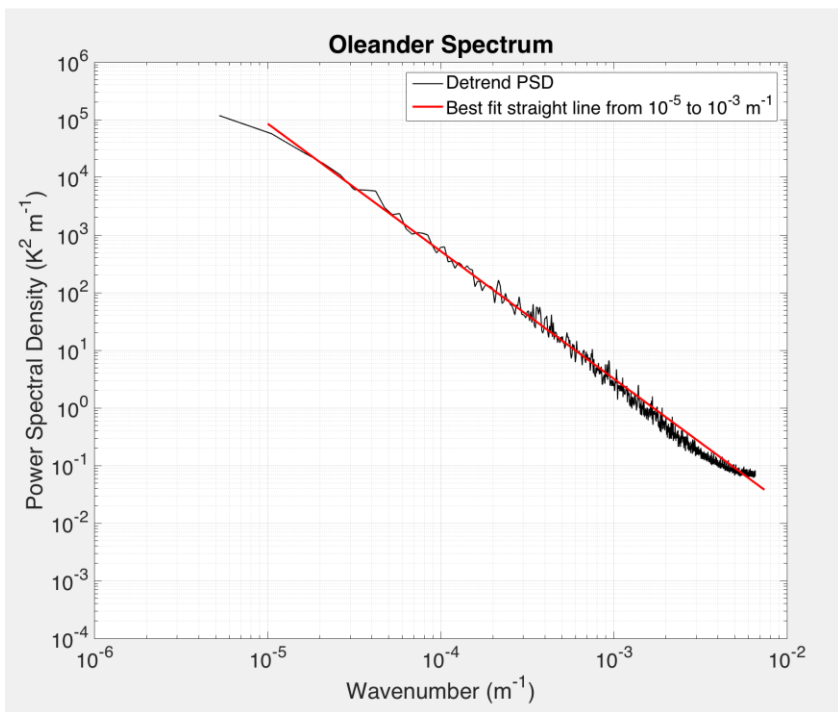
4.4 Comparison between the spectra of VIIRS and AVHRR SST fields



Along-scan



Along-track



Black curve: TEX spectra
Straight red line: least squares best fit straight line

TEX Spectra with noise added to



Spectra Approach:

- Three assumptions to determine the instrument noise:
 - 1) The \log_{10} of the geophysical power spectral density in the study area falls off linearly with \log_{10} of the wavenumber over the spectral range sampled by the satellite-borne sensors (1.5 km to 100 km).
 - 2) The spectrum continues to roll-off with approximately the same slope, at wavenumbers larger than those associated with the Nyquist frequency of the satellite temperature sections.
 - 3) The instrument noise for both sensors is white; i.e., that it contributes equally at all wavenumbers associated with the given temperature sections.
- Steps to estimate noise:

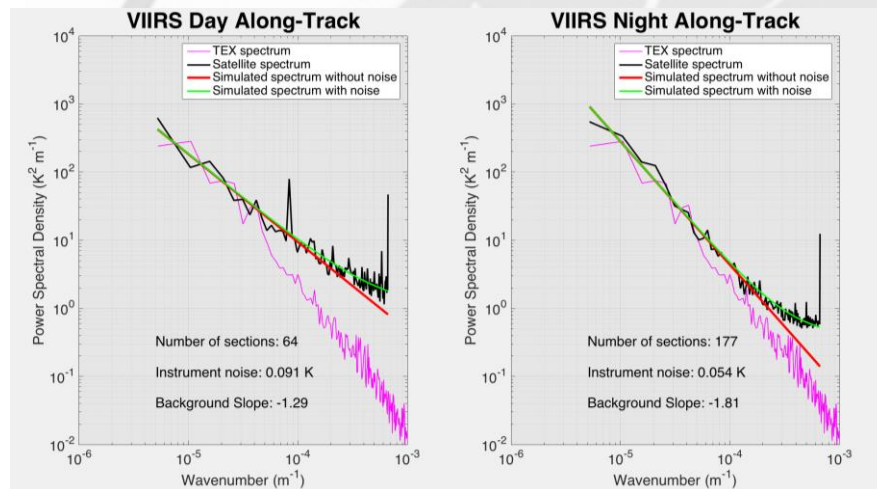
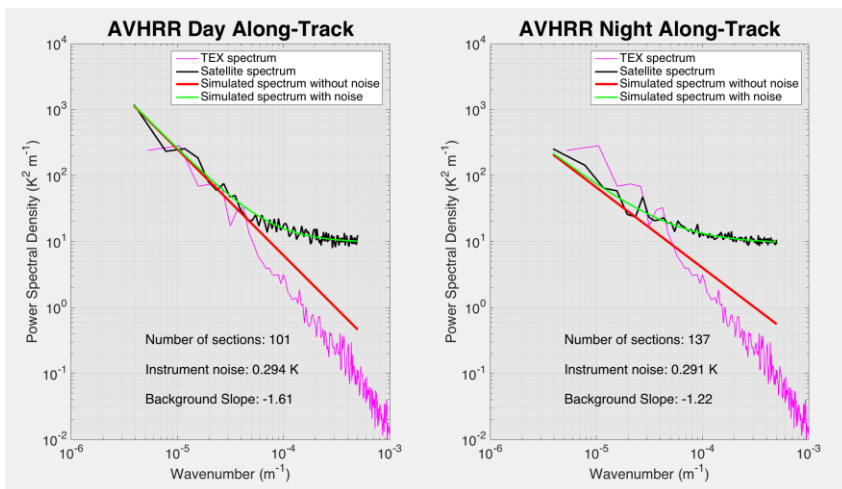
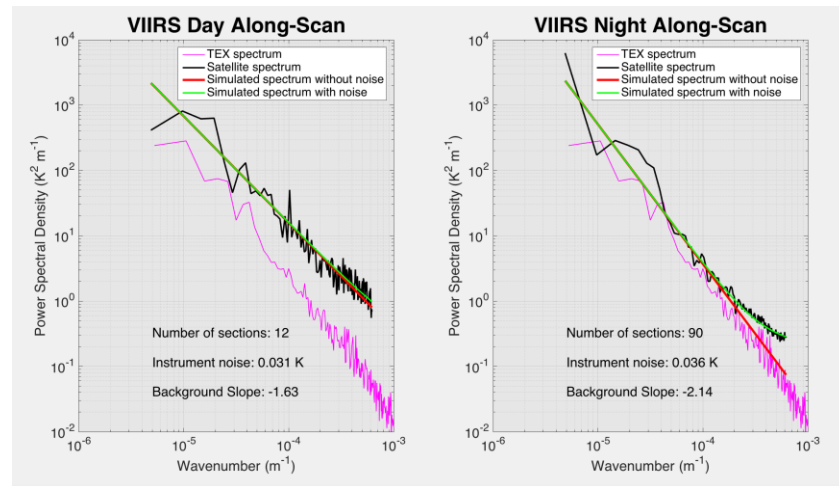
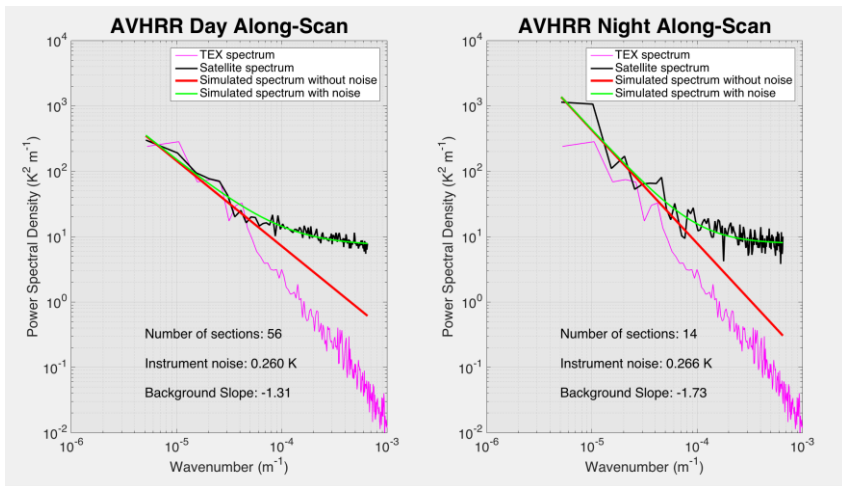
$$\gamma(\text{slope}, \text{intercept}, \text{noise}) = \sum_{i=1}^N \left(\left(10^{(\text{slope} \cdot \log_{10} k_i + \text{intercept})} + \text{noise} \right) - PSD_i^{\text{sat}} \right)^2$$



Best fit slope, intercept



$$\gamma(\sigma) = \sum_{i=1}^N \left(PSD_i^{\text{Simulated}}(\sigma) - PSD_i^{\text{Best fit}}(\text{slope}, \text{intercept}) \right)^2$$





Variogram approach:

$$\gamma(\Delta_{x \text{ or } y}) = \sigma_0^2 + \sigma^2(1 - e^{-\left(\frac{\Delta_{x \text{ or } y}}{L}\right)^w})$$

σ_0^2 : referred to as the nugget, is the variance of the difference in the retrieval at a given location from that at a neighboring location as the separation between the two locations goes to zero

σ^2 : the instrument noise in this case. It depends on the variance in the atmosphere, the variance of the surface emissivity, instrument noise, etc.

So,

$$\sigma^2 \approx \sigma_{geo}^2 + (\sigma_{retrieval}^2 - \sigma_0^2)$$

$$\hat{\gamma}(\Delta_{x \text{ or } y}) = \frac{\sum_{(s_i, s_j)} (SST(s_i) - SST(s_j))^2}{2n}$$



AVHRR:

Instrument Noise: 0.17 K ~ 0.22 K.

Daytime values were virtually identical to nighttime values.

The noise estimated by the 2 methods are similar.

VIIRS:

Instrument Noise: 0.02 K ~ 0.08 K on the scan geometry.

Daytime values $\approx 2 \times$ Nighttime values (Diurnal warming)

Along-track values $\approx 1.5 \times$ Along-scan values (multiple detectors banding)

The spectral approach is thought to be the more accurate (aliased energy at higher wavenumbers than those sampled are compensated for)

Estimated instrument noise in satellite-derived SST fields.

	Method	Day (K)		Night (K)	
		Along-Scan	Along-Track	Along-Scan	Along-Track
AVHRR Pathfinder	Spectra	0.172±0.001	0.209±0.001	0.173±0.003	0.209±0.008
	Variogram	0.185±0.004	0.219±0.006	0.183±0.001	0.219±0.006
	Upper Limit	0.189	0.218	0.194	0.208
VIIRS JPSS	Spectra	0.046±0.001	0.076±0.002	0.021±0.001	0.032±0.002
	Variogram	0.081±0.013	0.097±0.006	0.042±0.004	0.056±0.004
	Upper Limit	0.078	0.101	0.050	0.057

Upper Limit :
$$\sigma^2(\Delta x_{\min}) = 2\sigma_t^2 + \sigma_{geo}^2(\Delta x_{\min}) \Rightarrow \sigma_t \leq \frac{\sigma(\Delta x_{\min})}{\sqrt{2}}$$

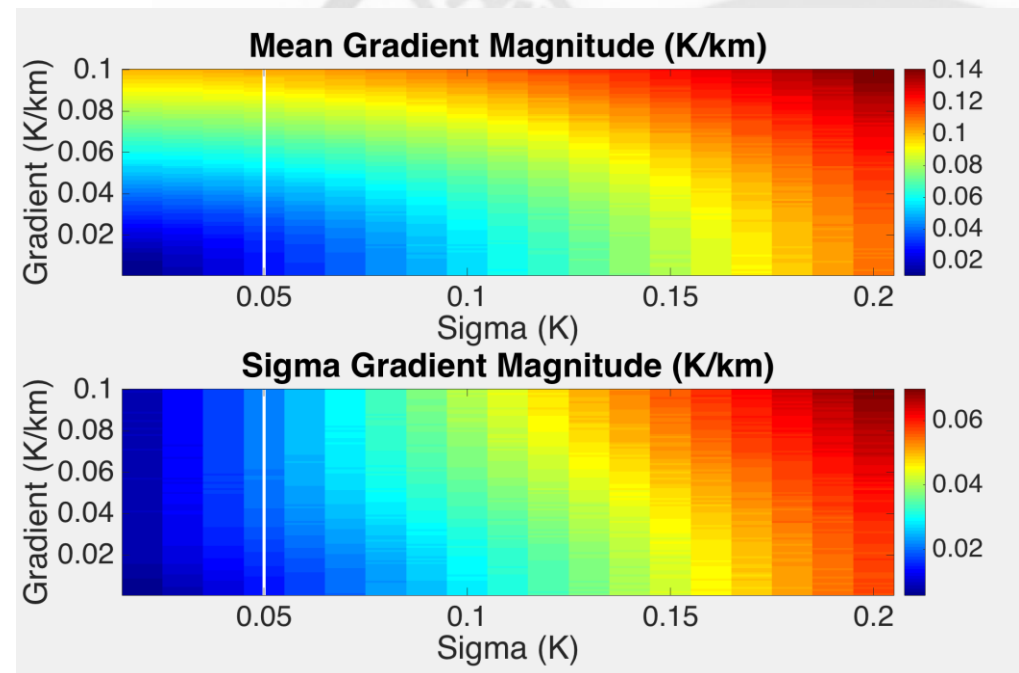


How does noise impact satellite-derived SST gradients?

- Simulate 10,000 3x3 pixel squares for a fixed gradient in x, 0 in y.
- Added Gaussian white noise to each of the elements.
- Applied the 3x3 Sobel gradient operator in x and.
- Determine the μ and σ of the resulting gradient components and the gradient magnitude
- Performed the above for:

$$0.01 \text{ K/km} < \frac{\partial T}{\partial x} < 0.1 \text{ K/km}$$

$$0.001 \text{ K} < \sigma < 0.2 \text{ K}$$





- Impact of noise on the Sobel Gradient.
- **The impact of noise on the determination of SST gradients:** On average
 - The mean noise of x- and y-components aren't affected by instrument noise.
 - The standard deviation of x- and y-components is approximately
 - $\frac{1}{2}$ of the imposed noise level
 - Independent of the underlying gradient.
 - The gradient magnitude for typical ocean gradients is
 - Accurately estimated with VIIRS
 - Substantially overestimated for AVHRR.
 - The standard deviation of gradient magnitude estimates:
 - Increases with the underlying gradient
 - But is in general smaller than that of the individual components;
- approximately 1/3 of the imposed noise.



- **Pixel-to-pixel noise in AVHRR and VIIRS L2 fields**
 - AVHRR noise (0.2 K) is significantly larger than VIIRS noise (0.05 K).
 - Along-track noise is larger than along-scan noise
 - Daytime levels are higher than nighttime levels.
 - For AVHRR, the two methods provide very similar results
 - For VIIRS, spectral estimates tend to be between 50% and 70% of those based on the variogram.
- **Which method to use to estimate instrument noise:**
 - The variogram for instruments with noise > 0.1 K;
 - it requires significantly less preprocessing than the spectral approach
 - For the higher quality instruments
 - The variogram provides an upper limit on the estimate
 - But needs work for a more accurate estimate.

